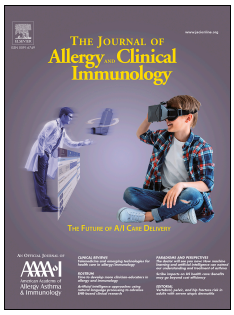
Journal Pre-proof



Aberrant inflammatory responses to type I interferon in STAT2 or IRF9 deficiency

Florian Gothe, MD, Jarmila Stremenova Spegarova, PhD, Catherine F. Hatton, MSc, Helen Griffin, PhD, Thomas Sargent, BSc, Sally A. Cowley, PhD, William James, DPhil, Anna Roppelt, MD, Anna Shcherbina, MD, Fabian Hauck, MD PhD, Hugh T. Reyburn, PhD, Christopher J.A. Duncan, DPhil, Sophie Hambleton, DPhil

PII: S0091-6749(22)00185-3

DOI: https://doi.org/10.1016/j.jaci.2022.01.026

Reference: YMAI 15461

To appear in: *Journal of Allergy and Clinical Immunology*

Received Date: 23 June 2021

Revised Date: 13 December 2021

Accepted Date: 14 January 2022

Please cite this article as: Gothe F, Spegarova JS, Hatton CF, Griffin H, Sargent T, Cowley SA, James W, Roppelt A, Shcherbina A, Hauck F, Reyburn HT, Duncan CJA, Hambleton S, Aberrant inflammatory responses to type I interferon in STAT2 or IRF9 deficiency, *Journal of Allergy and Clinical Immunology* (2022), doi: https://doi.org/10.1016/j.jaci.2022.01.026.

This is a PDF file of an article that has undergone enhancements after acceptance, such as the addition of a cover page and metadata, and formatting for readability, but it is not yet the definitive version of record. This version will undergo additional copyediting, typesetting and review before it is published in its final form, but we are providing this version to give early visibility of the article. Please note that, during the production process, errors may be discovered which could affect the content, and all legal disclaimers that apply to the journal pertain.

© 2022 Published by Elsevier Inc. on behalf of the American Academy of Allergy, Asthma & Immunology.

Journal Pre-proof

Aberrant inflammatory responses to type I interferon in STAT2 or IRF9 deficiency

Authors

Florian Gothe MD[1,2]

Jarmila Stremenova Spegarova PhD[1]

Catherine F. Hatton MSc[1]

Helen Griffin PhD[1]

Thomas Sargent BSc[1]

Sally A. Cowley PhD[3]

William James DPhil[3]

Anna Roppelt MD[4]

Anna Shcherbina MD[4]

Fabian Hauck MD PhD[2]

Hugh T. Reyburn PhD[5]

Christopher J. A. Duncan DPhil[1,6*]

Sophie Hambleton DPhil[1,7*]

1. Immunity and Inflammation Theme, Translational and Clinical Research Institute, Newcastle University, UK.

2. Department of Pediatrics, Dr. von Hauner Children's Hospital, University Hospital, Ludwig-Maximilians-Universität Munich, Munich, Germany.

3. James & Lillian Martin Centre for Stem Cell Research, Sir William Dunn School of Pathology, Oxford University, UK.

Journal Pre-proof

Journal Pre-proof

4. Department of Immunology, Dmitry Rogachev National Medical Research Center of Pediatric Hematology, Oncology and Immunology, Moscow, Russia.

5. Department of Immunology and Oncology, Spanish Center for Biotechnology, Madrid, Spain.

6. Infection and Tropical Medicine, Royal Victoria Infirmary, The Newcastle upon Tyne Hospitals NHS Foundation Trust, UK.

7. Children's Immunology Service, Great North Children's Hospital, The Newcastle upon Tyne Hospitals NHS Foundation Trust, UK.

* These authors contributed equally

Corresponding authors:

Professor Sophie Hambleton DPhil

Translational and Clinical Research Institute

Immunity & Inflammation Theme

Faculty of Medical Sciences

3rd Floor, Leech Building

Newcastle University Medical School

NE2 4HH

Newcastle upon Tyne

Telephone: +44 (0) 191 208 3850

Fax: +44 (0) 191 208 7179

Email: sophie.hambleton@ncl.ac.uk

Dr. Christopher J. A. Duncan DPhil

Translational and Clinical Research Institute

Immunity & Inflammation Theme

Journal Pre-proof

Journal Pre-proof

Faculty of Medical Sciences
3rd Floor, Leech Building
Newcastle University Medical School
NE2 4HH
Newcastle upon Tyne
Tel: +44(0)191 2087362
Fax: +44(0)191 2085455
Email: christopher.duncan@ncl.ac.uk

Funding:

FG is supported by the Munich Clinician Scientist Program at LMU (FoeFoLe^{plus}) and received fellowships from the Bubble Foundation as well as the Care-for-Rare Foundation. CFH is funded by an MRC studentship [MR/N013840/1]. FH is funded by the Else Kröner-Fresenius Stiftung (EKFS, 2017_A110) and the German Federal Ministry of Education and Research (BMBF, 01GM1910C). SH and CJAD are funded by the Wellcome Trust [207556/Z/17/Z and 211153/Z/18/Z respectively].

Conflict of interest statement:

SH declares honoraria from CSL Behring and Takeda for teaching and consultancy. The remaining authors declare no competing interests.

Journal Pre-proof

Journal Pre-proof

Abstract:

Background: Inflammatory phenomena such as hyperinflammation or hemophagocytic lymphohistiocytosis are a frequent yet paradoxical accompaniment to viral susceptibility in patients with impairment of type I interferon (IFN-I) signaling caused by deficiency of STAT2 or IRF9.

Objective: We hypothesized that altered and/or prolonged IFN-I signaling contributes to inflammatory complications in these patients.

Methods: We explored the signaling kinetics and residual transcriptional responses of IFN-stimulated primary cells from individuals with complete loss of either STAT1, STAT2 or IRF9 as well as gene-edited iPSC-derived macrophages.

Results: Deficiency of any ISGF3 component suppressed but did not abrogate IFN-I receptor signaling, which was abnormally prolonged in keeping with insufficient induction of negative regulators such as USP18. In cells lacking either STAT2 or IRF9, this late transcriptional response to IFNα2b mimicked the effect of IFNγ.

Conclusion: Our data suggest a model wherein the failure of negative feedback of IFN-I signaling in STAT2 and IRF9 deficiency leads to immune dysregulation. Aberrant IFNAR signaling in STAT2- and IRF9-deficient cells switches the transcriptional output to a prolonged, IFNγ-like response and likely contributes to clinically overt inflammation in these individuals.

Journal Pre-proof

Journal Pre-proof

Key messages:

- Cells deficient in components of the ISGF3 transcription factor complex (STAT1, STAT2, IRF9) display prolonged IFNAR signaling as a consequence of failure to initiate negative feedback regulation via USP18.
- In $STAT2^{-/-}$ and $IRF9^{-/-}$ cells, this dysregulated response leads to a sustained shift towards STAT1-dependent transcription, inducing in macrophages a functional state more closely resembling an IFN-gamma response.
- This aberrant inflammatory response provides one explanation for the clinical manifestations of hyperinflammation seen in patients with autosomal recessive deficiency of *STAT2* and *IRF9*.

Capsule summary:

Inflammatory complications are unexplained in STAT2- and IRF9-deficient patients. In STAT2- and IRF9-deficient cells, IFN-I triggers an aberrant, proinflammatory state resembling IFNγ activation, potentially contributing to the pathogenesis of clinical hyperinflammation.

Key words:

Type I interferon, antiviral immunity, ISGF3, HLH, type II interferon, GAF, STAT2, IRF9

Abbreviations:

CIITA	Class II major histocompatibility complex transactivator
CRISPR	Clustered regularly interspaced short palindromic repeats
CXCL	C-X-C motif chemokine ligand
EBV	Epstein Barr virus
GAF	Interferon γ activation factor

Journal Pre-proof

121	GAS	Interferon γ activated sites
122	GBP	Guanylate binding protein
123	HLH	Hemophagocytic lymphohistiocytosis
124	ICAM1	Intercellular adhesion molecule 1
125	HLA-DR	Human leukocyte antigen – DR isotype
126	IFN	Interferon
127	IFNAR	Interferon α receptor
128	iPSC	Induced pluripotent stem cells
129	IRF	Interferon regulatory factor
130	ISG	Interferon stimulated gene
131	ISGF3	Interferon stimulated gene factor 3
132	ISRE	Interferon-sensitive response element
133	JAK	Janus tyrosine kinase
134	KO	Knock-out
135	LCL	Lymphoblastoid cell line
136	MHC	Major histocompatibility complex
137	SOCS	Suppressor of cytokine signaling
138	STAT	Signal transducer and activator of transcription
139	TLR	Toll-like receptor
140	USP18	Ubiquitin specific peptidase 18
141	WT	Wild type

Journal Pre-proof

Journal Pre-proof

Introduction:

Interferons (IFN) constitute an important and well-studied anti-viral defense system in mammalian immunity(1). Almost every human cell type is capable of both producing and responding to type I IFN (IFN-I, various subtypes of IFNα and IFNβ) in the face of viral challenge. Conversely, the production of type II IFN (IFNγ), a potent immunostimulatory cytokine, is tightly regulated and confined to specific lymphocyte subsets. All IFNs, including the mucosa-restricted type III IFNs, employ the Janus tyrosine kinase (JAK) – signal transducer and activator of transcription (STAT) pathway to influence gene expression. In the canonical model of signaling downstream of the IFNα receptor (IFNAR), a heterotrimeric transcription factor complex is formed, consisting of tyrosine phosphorylated STAT1 and STAT2 together with interferon regulatory factor 9 (IRF9), and known as interferon stimulated gene factor 3 (ISGF3). A fraction of phosphorylated STAT1, however, homodimerizes to form the IFNγ activation factor (GAF), agonizing a partially overlapping set of interferon-stimulated genes (ISG), typically induced following type II IFN signaling via the IFNγ receptor(1). To restrain this potent proinflammatory response, robust negative feedback mechanisms are simultaneously induced by ISGF3 to terminate further IFNAR signaling. Failure of this negative feedback mechanism results in life-threatening IFN-mediated inflammatory disease(2–5).

In recent years, severe viral susceptibility has been recognized as the shared clinical feature of monogenic inborn errors of IFN-I immunity resulting from biallelic deficiency of IFNAR, STAT1, STAT2 or IRF9(6–9). In parallel, unexplained inflammatory phenotypes such as prolonged virus-induced or sterile hyperinflammation(10) or even hemophagocytic lymphohistiocytosis (HLH)(9,11) have been noted in STAT2- and IRF9-deficient individuals, as in other defects of IFN-I immunity(12–14). HLH is a state of severe, systemic hyperinflammation associated with excessive production of IFNγ(15) and often triggered by persistent viral replication in the face of an ineffective antiviral immune response. In the case

of STAT2 and IRF9 deficiency, episodes of hyperinflammation have been reported in the absence of viral infection(9,10).

Here, we consider the possibility that inflammation might arise in STAT2- or IRF9-deficient patients due to prolonged and/or altered IFNAR signaling. We provide evidence that aberrant IFNAR signaling in STAT2- and IRF9-deficient cells mimics the effects of IFNγ stimulation, offering the potential for new therapeutic strategies in managing this life-threatening inflammatory state.

Journal Pre-proof

Journal Pre-proof

Methods:

The study was conducted according to the principles expressed in the Declaration of Helsinki and approved by the Newcastle and North Tyneside Research Ethics Committee, and the Institutional Research Ethics Committees of LMU Munich, Dmitry Rogachev National Medical Research Moscow and La Paz University Hospital.

Cells, cytokines and inhibitors

Primary EBV-LCLs from a previously described patient with complete, autosomal-recessive *STAT1* deficiency (p.V339Pfs*18)(13), an unreported patient with complete *STAT2* deficiency (compound heterozygous for two large deletions affecting STAT2: Chr12:56360796-Ch12:56352109 and Chr12:56355504-Ch12:56348082) and two siblings with complete *IRF9* deficiency (homozygous c.577+1G>T)(9) were cultured in RPMI medium supplemented by 10% fetal calf serum (FCS), 1% penicillin/streptomycin and 1% L-Glutamine (all from Gibco). Cytokines were used at the following concentrations: human recombinant IFNα2b (1000 IU/ml; Intron A, Schering-Plough, USA); IFNγ (1000 IU/ml; Immunikin, Boehringer Ingelheim, Germany); IL-4 (50 ng/mL, Peprotech, USA); IL-5 (50 ng/mL, Peprotech, USA), IL-13 (50 ng/mL, Peprotech, USA), Dexamethasone (10 uM, Organon Laboratories Limited, USA); Ruxolitinib (1 uM, S1378, Calbiochem, USA).

Immunoblotting

10^6 EBV-LCLs were washed in phosphate-buffered saline and lysed on ice in lysis buffer [50 mM Tris-HCl (pH 7.5), 150 mM NaCl, 1% Nonidet P-40, 0.1% SDS, 0.5% Na-Deoxycholate] containing 100 mM dithiothreitol (Sigma-Aldrich), 1× complete protease inhibitor cocktail (Roche, Basel, Switzerland), 1x PhosSTOP phosphatase inhibitors (Roche), and 1× NuPAGE Loading Buffer (Life Technologies). Lysates were heated to 70°C for 10 min before being subjected to 4 to 12% tris-glycine polyacrylamide gel (Novex, Life Technologies)

Journal Pre-proof

electrophoresis in 1×SDS NuPAGE MOPS Running Buffer (Life Technologies) with Prestained Plus Protein Ladder (Thermo Scientific) as molecular weight markers. Proteins were transferred to 0.45-mm polyvinyl difluoride membranes (Thermo Scientific) in NuPAGE Tris-Glycine Transfer Buffer. Membranes were blocked for 60 min in 5% bovine serum albumin in tris-buffered saline with 0.1% Tween (TBS-T) before immunostaining by standard methods. A list of anti-human antibodies used together with appropriate horseradish peroxidase (HRP)–conjugated secondary antibodies can be found in Table S1. Membranes were washed in TBS-T and developed with Immobilon Western Chemiluminescent HRP substrate (Millipore) and imaged on a LI-COR Odyssey Fc (LI-COR).

Phospho-flow

$2x10^5$ EBV-LCLs cells were seeded in 200 µl serum-free X-VIVO 15 medium (Lonza, Basel, Switzerland) and stimulated with IFNα2b for the indicated times. In case a restimulation with IFNγ was planned, cells were extensively washed to remove any IFNα2b after the priming period and cells were rested for three hours to allow pSTAT1 levels to return to baseline. After staining with Zombie UV (BioLegend, San Diego, CA, USA), cells were fixed using Cytofix buffer (BD Biosciences, Franklin Lakes, NJ, USA). Permeabilization was achieved by adding ice-cold PermIII buffer (BD Biosciences, Franklin Lakes, NJ, USA), and cells were incubated on ice for 20 min. After repeated washing steps with phosphate-buffered saline (PBS)/2% fetal bovine serum (FBS), cells were stained for 60 min at room temperature with directly conjugated antibodies (Table S2). Samples were acquired on a Symphony A5 flow cytometer (BD Biosciences) and analyzed using FlowJo (FlowJo LLC, Ashland, OR, USA). The gating strategy can be found in Fig. S1a.

qRT-PCR

Journal Pre-proof

RNA was extracted using the ReliaPrep RNA Cell Miniprep System (Promega) and equal amounts were reverse-transcribed with Superscript III (ThermoFisher Scientific). The resulting cDNA templates were subjected to qPCR with a TaqMan™ Gene Expression Master Mix (Applied Biosystems) according to manufacturer's instructions. Primers and related probes used were designed by Roche Universal Probe Library System Assay Design (Roche, Basel, Switzerland) and are included in Table S3. Plates were run on an AriaMx Real-time PCR System (Agilent Technologies).

Immunoprecipitation

EBV-LCLs were stimulated with IFNα2b for 15 min, washed with ice-cold PBS and lysed in RIPA buffer [50 mM Tris (pH 7.5), 1 mM EDTA, 150 mM NaCl, 1% Nonidet P-40, 0.1% SDS, 0.5% Na-Deoxycholate, 1 × complete protease inhibitor cocktail (Roche, Basel, Switzerland) and 1x PhosSTOP phosphatase inhibitors (Roche)]. Lysates were centrifuged at 13,000 rpm at 4°C for 10 min. Soluble fractions were pre-cleared for 1 hour at 4°C with Protein G Sepharose 4 Fast Flow beads (GE Healthcare, Chicago, USA) that had been previously blocked with 1% bovine serum albumin (BSA) containing wash buffer [50 mM Tris (pH 7.5), 1 mM EDTA, 150 mM NaCl, 1% Nonidet P-40, 1x complete protease inhibitor cocktail (Roche, Basel, Switzerland) and 1x PhosSTOP phosphatase inhibitors (Roche)] for 1 hour. Precleared cell lysates were immunoprecipitated overnight with blocked beads that were incubated with anti-STAT1a antibody (C-111) or anti-STAT2 antibody (A-7) for 1 hour and then washed four times in before boiling with 4× lithium dodecyl sulfate buffer at 95°C for 10 min to elute the absorbed immunocomplexes. Immunoblot was carried out as described above.

Gene editing and iPSC differentiation

The parental iPSC line (SFC856-03-04) used for CRISPR editing, generated from a healthy adult donor at the University of Oxford, has been described previously(16), is registered in

Journal Pre-proof

https://hpscreg.eu/ and is available from https://ebisc.org/. For gene editing the Alt-R CRISPR-Cas9 system (IDT) was used aiming to induce gene deletions that (i) remove exon-intron boundaries (for *STAT1* and *IRF9*) or (ii) led to a frameshift (*STAT2*), thereby causing gene ablation through nonsense mediated mRNA decay. The guide RNAs used are listed in Table S4. To introduce guide RNAs alongside a tracrRNA as well as the Cas9 enzyme, the Neon transfection system (Thermo Fisher) was used. After transfection of the iPSC pool, cells were plated at low density on irradiated mouse embryonic fibroblasts to allow single cell colonies to grow. Individual colonies were picked after 7 days under the microscope and expanded in 96 well plates. The success of gene editing was assessed by immunoblot for STAT1 and STAT2. Since IRF9 is not expressed in iPSC, clones were analyzed by nucleotide sequencing using the following primers: TAGCGGTGCATGCCTGTAG and AGCAAGGACAGAGGGTGAAG (Fwd-Rev). The differentiation process was carried out following the protocol published by van Wilgenburg *et al.*(17). In brief, iPSCs were seeded on AggreWell 800 plates (Stemcell Technologies) at a density of $4x10^6$/mL. Embryoid bodies were harvested at day 4 and transferred into T175 flasks containing X-VIVO 15 medium (Lonza), supplemented with M-CSF (100 ng/mL) and IL-3 (25 ng/mL, both purchased from Invitrogen). After several weeks with weekly media changes, macrophage precursors could be harvested. These were plated at a density $2x10^5$ cells/mL and terminally differentiated in X-VIVO 15 medium containing M-CSF in the abovementioned concentration. After 7 days, macrophages were ready to be used for experiments. To confirm that the differentiated cells express key features of macrophages, analysis of different cell surface markers was assessed by flow cytometry and a phagocytosis assay was carried out as described below. Additionally, STAT1, STAT2 and IRF9 were assessed by immunoblot to ensure knock-out of the specific protein.

Flow cytometry

Journal Pre-proof

Macrophages were lifted using PBS containing 5 mM EDTA and washed with PBS/2% FCS. EBV-LCL were also washed using PBS/2% FCS. Cells were stained with surface markers for 30 min at room temperature (a list of directly conjugated antibodies can be found in Table S5). To validate expression of various macrophage markers, appropriate isotype controls were used. When intracellular markers were investigated, cells were fixed using Cytofix buffer (BD) and permeabilized with Cytoperm (BD) according to the manufacturer's instructions. Intracellular staining was performed for 30 minutes at 4°C in the dark. Samples were acquired on a Symphony A5 flow cytometer (BD Biosciences) and analyzed using FlowJo v10.2 (FlowJo LLC, Ashland, OR, USA). The gating strategy is exemplified in Fig. S1b.

Phagocytosis assay

$2x10^5$ macrophages were lifted and placed in Eppendorf tubes containing fresh X-VIVO 15 medium. pHrodo Red A Zymosan bioparticles (Invitrogen) were then added at a ratio of 10:1 cells. The negative control was immediately placed on ice, whereas the positive control was put into a shaking incubator for 2 hrs at 37°C. Phagocytosis was terminated by placing the cells on ice. Macrophages were subsequently transferred to FACS tubes and 4',6-diamidino-2-phenylindole (DAPI, ThermoFisher Scientific) was added before acquiring cells on a BD Symphony Flow cytometer. Data was analyzed using FlowJo.

Cytokine production assay in macrophages

Macrophages were plated at a density of $2x10^5$ cells/mL and preincubated with either IFNα2b or IFNγ at a concentration of 1000 IU/mL for 48 hrs or left untreated. As a second stimulus, LPS was added at a final concentration of 100 ng/mL and cells were further incubated for another 6 hrs. Brefeldin A (Biolegend) was added to allow intracellular accumulation of cytokines under investigation. Cells were lifted using 5 mM EDTA and stained with antibodies against TNFα and as stated in the flow cytometry section.

Journal Pre-proof

Nanostring analysis

RNA was extracted by lysing macrophages in TRIzol reagent (Thermo Fisher Scientific) as previously described and stored at -80°C until analyzed. RNA was purified using the RNA Clean and Concentrator-5 kit (Zymo Research) before 100 ng of total RNA were loaded onto the Nanostring nCounter cartridge following the manufacturer's instructions. Raw data files were imported into the nSolver 4.0 software. All samples passed quality control assessment. Data normalization included positive control normalization as well as mRNA content normalization based on the expression of the housekeeping genes *ABCF1*, *GUSB*, *MRPS7*, *NMT1*, *NRDE2*, *OAZ1*, *PGK1*, *SDHA* and *TBP*. Log2-transformed expression or ratio data were exported and visualized using GraphPad Prism version 9.0.2 (GraphPad Sofware Inc.). Differentially expressed genes were analyzed for overrepresented conserved transcription factor binding sites in the promoter sequence (±10,000 bases) by single site analysis by using oPOSSUM database 3.0(18) with a conservation cutoff of 0.4 and matrix score threshold of 85%. Promoters were examined for the presence of ISGF3 (ISRE), IRF1, and STAT1 (GAS) binding sites. For the pathway analysis, the ConsensusPathDB interaction database (http://consensuspathdb.org/)(19) was used to identify genes with significantly different expression after 48 hrs of stimulation with IFNα2b (1000 IU/mL). Genes were then referenced against the Gene Ontology (GO) resource(20) GO terms were ranked based on their respective Q values when compared to WT cells.

Statistical analysis

Unless otherwise stated, all experiments were repeated a minimum of three times. Data were normalized/$\log_{10}$-transformed before parametric tests of significance in light of the limitations of ascertaining distribution in small sample sizes and the high type II error rates of nonparametric tests in this context. Comparisons of more than one group used one-way analysis

Journal Pre-proof

of variance (ANOVA) with Tukey correction for multiple comparisons. Statistical testing was undertaken in GraphPad Prism (version 9.0.2). Two tailed P values < 0.05 were considered statistically significant.

Journal Pre-proof

Journal Pre-proof

Results:

Prolonged IFNAR signaling in ISGF3 component-deficient cells

We first examined the kinetics of IFNAR signaling by probing phosphorylation of JAK-STAT molecules in cells stimulated with IFN-I. Studies to date have focused on early events in ISGF3-deficient cells(6–8), but here we sought to examine responses over a longer period, testing the prediction that defects in the induction of ISGF3-dependent negative regulation would lead to prolonged activation of the remaining JAK-STAT molecules. Epstein Barr virus (EBV)-transformed B-lymphoblastoid cell lines (LCLs) were generated from patients with ISGF3-component deficiencies and stimulated with IFNα2b for up to 48 hrs (Fig. 1). Immunoblotting confirmed that patient EBV-LCLs were null for either STAT1, STAT2 or IRF9 and often showed secondarily reduced expression of other ISGF3 components at baseline (Fig. 1a). This is consistent with the fact that *STAT1*, *STAT2* and *IRF9* are themselves ISGs, and their expression is positively regulated by 'tonic' expression of IFN-I(21). By contrast, JAK1 expression was preserved in ISGF3 deficient cells. In these EBV-transformed cell lines, we saw some evidence of basal IFN signaling in the form of constitutive phosphorylation of JAK1 and residual ISGF3 components (Fig. 1a and b).

After 1 hour of IFNα2b stimulation, robust JAK1 phosphorylation was observed in healthy control cells as well as the different patient cell lines (Fig. 1a). However, the induction of STAT2 phosphorylation in $STAT1^{-/-}$ cells and pSTAT1 in $STAT2^{-/-}$ cells were significantly reduced at this early timepoint relative to control (Fig. 1c and d), due to reductions in total cellular STAT. In $IRF9^{-/-}$ cells, conversely, STAT1 and STAT2 were phosphorylated at similar levels as in control cells. By 6 hrs of stimulation, JAK1 phosphorylation was hardly visible in control cells (Fig. 1a) and both pSTAT1 and pSTAT2 had already decreased to levels only slightly above baseline (Fig. 1c and d), reflecting appropriate negative feedback on IFNAR. In marked contrast, JAK1 phosphorylation persisted in all ISGF3 component-deficient cells until at least 24 hrs (Fig. 1a), indicative of persistent proximal signaling in the absence of ISGF3

Journal Pre-proof

components and the failure of negative feedback. Consistent with this, STAT2 phosphorylation remained elevated for up to 48 hrs of stimulation in both STAT1$^{-/-}$ and IRF9$^{-/-}$ cells (Fig. 1d). A similar phenomenon was also seen in pSTAT1 levels in STAT2- or IRF9-deficient cells (Fig. 1c), and although both STAT2- and IRF9-deficient cells showed some degree of signal attenuation after 6 hrs, pSTAT1 in STAT2$^{-/-}$ cells showed a secondary increase persisting to 48 hrs. In IRF9$^{-/-}$ cells, pSTAT1 remained consistently elevated between 6 and 48 hrs. In summary, IFNα2b stimulation of cells lacking any ISGF3 component led to prolonged proximal signaling via IFNAR, albeit with differences in the kinetic and magnitude of STAT phosphorylation between the different deficient cell lines.

Failure of USP18-induced negative regulation

We hypothesized that prolonged IFNAR signaling might reflect a failure of negative feedback and proceeded to investigate the induction of relevant negative regulators. We focused on ubiquitin-specific protease 18 (USP18), which plays an essential role in suppressing IFN-I signaling(22) via displacement of JAK1 from IFNAR2 and prevention of downstream phosphorylation. Whereas *USP18* mRNA expression peaked after 24 hrs (Fig. 1e) in control cells, all ISGF3-deficient cell lines showed severely impaired *USP18* induction. Although some residual transcription was detectable in STAT1$^{-/-}$ cells, possibly reflecting the ability of residual STAT2:IRF9 containing complexes to mediate the expression of certain interferon-sensitive response element- (*ISRE-)* containing ISGs in the absence of STAT1(23,24), no induction of *USP18* could be observed in STAT2$^{-/-}$ or IRF9$^{-/-}$ cells, even as late as 48 hrs after onset of IFNα2b stimulation. We confirmed the preserved interaction of STAT2:IRF9 in STAT1$^{-/-}$ cells by immunoprecipitation (Fig. S2a). In contrast to previous reports(25), STAT1 and IRF9 did not appear to interact in the absence of STAT2 when assessed by this method (Fig. S2b). The observed defect of USP18 induction upon IFNα2b stimulation was also evident at the protein level in STAT2- and IRF9-deficient cells (Fig. 1a). This biochemical phenotype recalls that

Journal Pre-proof

seen in USP18-deficient cells(5) or cells with mutations in STAT2 that fail to support the regulatory action of USP18(2,3), suggesting that defective USP18-dependent feedback was responsible for prolonged IFNAR signaling in ISGF3-deficient cells.

Members of the suppressor of cytokine signaling (SOCS) group of proteins are also capable of inhibiting JAK-STAT signaling by directly suppressing the JAK kinase domain(26), although this activity fails to compensate for the loss of USP18 regulation in humans(2) or mice(27). *SOCS1* and *SOCS3* are known to be potently induced upon IFN stimulation(28) and indeed we saw preserved or even enhanced transcriptional induction of these regulators in ISGF3-component deficient cells (Fig. S3a and S3b). This induction of *SOCS* expression led to functional regulatory activity upon IFNγ signaling in WT and IRF9 deficient cells (Fig. S3c), although pSTAT1 responses were generally attenuated in STAT2-deficiency (and absent in STAT1-deficient cells included as a negative control). Thus, although SOCS activity was induced in ISGF3-deficient cells, this did not compensate for the defect of negative regulation of IFNAR signaling.

<u>GAS-dominated transcriptional output in STAT2$^{-/-}$ and IRF9$^{-/-}$ cells</u>

Next, we investigated the transcriptional changes associated with such altered IFNAR signaling. As with expression of *USP18,* the induction of ISGs such as *MX1* (Fig. 2a), *RSAD2* (Fig. 2b) or *IFI44L* (Fig. 2c) was absent from all ISGF3-deficient cells, thus confirming that ISGF3 drives the typical transcriptional response to IFN-I and in keeping with the viral susceptibility seen in these patients. In STAT2$^{-/-}$ and IRF9$^{-/-}$ cells, however, IFN-triggered formation of pSTAT1 homodimers (known as the gamma interferon activation factor [GAF]) would be expected to be preserved. We therefore explored the transcriptional activation of genes harboring GAS-elements. In keeping with our previous analysis at 10 hrs after IFNα2b stimulation of STAT2-deficient cells(7), we noted exaggerated induction of *IRF1* transcripts after 24 hrs in both STAT2$^{-/-}$ and IRF9$^{-/-}$ cells (Fig. 2d). Extending our analysis to other

Journal Pre-proof

410 classically IFNγ-induced genes, we found increased transcription of *CIITA*, the master regulator
411 of MHC class II expression in antigen-presenting cells, especially at later time points (Fig. 2e).
412 The same was true for *ICAM1*, encoding a protein expressed on macrophages and lymphocytes
413 that facilitates cell-cell interaction including immune synapse formation (Fig. 2f). We
414 confirmed the respective changes in the expression level of these markers following 48 hrs of
415 IFNα2b stimulation (Fig. S4).

Journal Pre-proof

Journal Pre-proof

Similar signaling kinetics in STAT2- and IRF9-knockout macrophages

To confirm and extend our findings in a cell type more relevant to hyperinflammation *in vivo*, we employed a model of macrophages derived from induced pluripotent stem cells (iPSC). We used CRISPR/Cas9 technology to knock out (KO) *STAT1*, *STAT2* or *IRF9* in a well-characterized iPSC line, and selected gene-edited and isogenic wild type (WT) control clones for experiments. These were differentiated to iPS-macrophages using a well-defined protocol(17). Analysis of the iPS-macrophages confirmed successful KO of the respective ISGF3 component, but preserved expression of classical macrophage surface markers as well as phagocytic activity (Fig. 3a-c). Details of the differentiation protocol and functional validation can be found in the methods section as well as in Fig. S5.

Interestingly, the basal JAK-STAT phosphorylation observed in ISGF3-deficient EBV-LCLs was absent from these untransformed cells. Stimulation with IFNα2b for up to 48 hrs induced similar kinetics of STAT phosphorylation as seen in the EBV-LCLs with prolonged activation of JAK1 and residual ISGF3 components. Again, we saw a complete lack of USP18 expression in $STAT2^{-/-}$ and $IRF9^{-/-}$ macrophages. Notably, some USP18 induction was observed in IFNα2b-stimulated $STAT1^{-/-}$ cells, together with delayed and reduced expression of antiviral proteins MX1, RSAD2 and ISG15 (Fig. 3a), all of which were completely absent from STAT2- and IRF9-deficient cells. These data confirm earlier observations in EBV-LCLs, consistent with reports that STAT2:IRF9 complexes mediate low-level ISG transcription in STAT1-deficient cells(24).

Transcriptional changes in $STAT2^{-/-}$ and $IRF9^{-/-}$ macrophages reveal an IFNγ-like pattern and altered time-course

Journal Pre-proof

To profile transcriptional changes in stimulated KO iPS-macrophages over time, we utilized the Nanostring Host Response Panel including 785 genes relevant to immune functions. Fig. S6 displays differentially expressed genes at baseline, confirming the reduction in basal expression of several ISGs as a consequence of the loss of STAT2, IRF9 or STAT1. After 1 hr of IFNα2b stimulation, all three KO lines displayed a marked failure to upregulate ISGs when compared to wild-type cells, with STAT2$^{-/-}$ and IRF9$^{-/-}$ cells showing a strikingly similar pattern (Fig. 4a). Conversely, the response to IFNγ was preserved in STAT2$^{-/-}$ and IRF9$^{-/-}$ cells, with STAT1$^{-/-}$ iPS-macrophages serving as a negative control in this experimental setting (Fig. S7). The previously observed failure of negative regulation became evident when comparing the transcriptional response at 1 and 48 hrs of IFNα2b stimulation (Fig. 4b). Whereas in WT cells, most of the initially upregulated genes show decreasing expression after 48 hrs, STAT2$^{-/-}$ and IRF9$^{-/-}$ cells again showed a distinct pattern with a larger transcriptional response at the later time point. This delayed response to IFN-I was also qualitatively different in STAT2$^{-/-}$ and IRF9$^{-/-}$ iPS-macrophages, with principal component analysis revealing the induction of an IFNγ-like transcriptional profile (Fig. 4c). Analysis of the promoter regions of genes differentially expressed in STAT2$^{-/-}$ and IRF9$^{-/-}$ cells compared to WT following 48 hrs of IFNα2b stimulation revealed a trend towards enrichment of GAS or IRF1-binding motifs compared to WT cells (Fig. 4d). Accordingly, among the pathways upregulated in STAT2$^{-/-}$ and IRF9$^{-/-}$ iPS-macrophages after 48 hrs of IFNα2b stimulation compared to WT were IFNγ signaling, antigen processing and presentation, the immune response to tuberculosis and proteasomal degradation, more typically associated with type II than IFN-I responses (Fig. S8). Interestingly, WT and STAT1$^{-/-}$ responses to IFNα2b grouped more closely on principal component analysis, which is in line with the immunoblot data showing preserved low-level induction of antiviral ISGs in the absence of STAT1 (Fig. 3a). We further profiled different cytokines implicated in HLH pathogenesis and observed increased transcription of *TNF*, *IL1B* and *IL6* in STAT2-and IRF9-deficient cells (Fig. S9).

Journal Pre-proof

Increased macrophage activation and TNFα production in STAT2$^{-/-}$ and IRF9$^{-/-}$ cells

To test whether the transcriptional shift towards an IFNγ-like output translates to the protein level, and to consider the wider impact on macrophage activation, the upregulation of activation markers was assessed by flow cytometry (Fig. 5a-d). In control cells, IFNα2b stimulation for either 24 or 72 hrs did not impact expression levels of HLA-DR, ICAM1 or IRF1. With IFNγ treatment, an increase over time was visible in all three of these markers (Fig. 5a-c). In STAT2$^{-/-}$ and IRF9$^{-/-}$ cells, however, IFNα2b stimulation led to increased marker expression, comparable to that seen with IFNγ stimulation of WT or mutant cells. As expected, STAT1$^{-/-}$ cells, used as a negative control, did not show substantial changes with either IFNα2b or IFNγ stimulation.

Furthermore, we assessed inflammatory cytokine production after priming macrophages with either IFNα2b or IFNγ for 48 hrs, using lipopolysaccharide (LPS) as the second stimulus (Fig. 5d). It has been well appreciated that IFNγ primes macrophages for enhanced responsiveness to Toll-like receptor (TLR) ligands and greatly augments TLR-induced expression of inflammatory cytokines(29). In both STAT2$^{-/-}$ and IRF9$^{-/-}$ macrophages, TNFα production was increased to an equivalent degree after priming with either IFNα2b or IFNγ. This increased TNFα production after IFNα2b exposure mimicked IFNγ responses in WT cells. IL-6 production, however, was not significantly enhanced in ISGF3 component-deficient iPS-derived macrophages over the levels in WT cells (Fig. S10). Interestingly, the upregulation of ICAM1, IRF1, and HLA-DR, also recapitulated in EBV-LCLs, could be prevented by dexamethasone as well as ruxolitinib treatment but was unaffected by pre-exposure to Th2 cytokines (Fig. S11a-c and Fig. S11d-f).

Journal Pre-proof

Discussion:

In this study, we propose a contributary mechanism for hitherto unexplained inflammatory complications in STAT2$^{-/-}$ and IRF9$^{-/-}$ individuals. Besides the well-studied defect in initiating an antiviral state, our data indicate a delayed, altered and dysregulated inflammatory response to IFN-I. Prolongation of ISGF3-independent IFNAR signaling, enabled by a failure to upregulate negative feedback inhibition via USP18, produces (i) a sustained shift towards GAF-driven transcription and (ii) a functional state resembling a type II IFN response in macrophages, likely contributing to aberrant inflammation.

In healthy individuals, the inflammatory response to IFN-I is held in check by powerful negative feedback upon proximal IFNAR signaling. A key finding of our studies in cells that lack ISGF3 components is that JAK-STAT activation in response to IFN-I is pathologically prolonged. A similar effect was previously described in mouse models of STAT1, STAT2 and IRF9 deficiency(30–32) and tentatively ascribed to insufficient early induction of *Socs1* transcription, known to interfere with Tyk2(33). However, evidence including the clinical phenotype of their respective human deficiency states now indicates that USP18 plays the dominant role in negative regulation of IFNAR signaling(5,34). USP18 is transcriptionally induced by ISGF3 and functions by sterically inhibiting the interaction of IFNAR2 and JAK1, in complex with STAT2(22,35). Accordingly, mutations in *USP18* and *ISG15*, the latter of which functions in stabilizing USP18, have been found to cause type I interferonopathy by abrogating the down-regulation of late IFN-I responses(4,5). When USP18 function is inhibited as a consequence of perturbed interaction with STAT2, unrestrained IFN signaling is again observed(2,3). Further experimental evidence corroborating the key role of USP18 is provided by Taylor and co-workers: both in human monocyte-derived macrophages where *USP18* has been knocked down as well as in iPSC-derived macrophages with *USP18* knockout, prolonged STAT1 and STAT2 signaling were observed after stimulation with IFN-I for 18 hrs(36). The

Journal Pre-proof

observed failure to robustly upregulate USP18 in STAT1$^{-/-}$, STAT2$^{-/-}$ and IRF9$^{-/-}$ cells is therefore likely sufficient to explain prolonged IFNAR signaling.

As well as this delayed time-course we observed a qualitatively altered macrophage transcriptional response to IFNα2b in the context of STAT2 or IRF9 deficiency, towards that produced by IFNγ stimulation. This shift from IFN-I to IFN-II responses was reflected functionally in the heightened expression of macrophage activation markers such as IRF1, ICAM1 or HLA-DR as well as increased production of TNFα, a classical proinflammatory cytokine, which was comparable following IFNα2b or IFNγ in STAT2$^{-/-}$ and IRF9$^{-/-}$ macrophages. Consistent with our data, previous reports have described upregulation of MHC class II in *Stat2*$^{-/-}$ murine BMMs treated with IFNα(30), and adoption of an IFNγ-like transcriptional state in IFNα exposed *Stat2*$^{-/-}$ and *Irf9*$^{-/-}$ mixed glial cells(32). Importantly, these IFN-I dependent effects could be suppressed by treatment with dexamethasone, suggesting a potential therapeutic option in STAT2- or IRF9-deficient patients with hyperinflammation.

Our data confirm that the aberrant signaling shared by STAT2- and IRF9-deficient cells in response to IFN-I is distinct from STAT1-deficient cells, evidence that the switch to an IFNγ-like transcriptional output is dependent on expression of STAT1. Based on our experiments in EBV-LCLs, it is also tempting to conclude that there may be enhanced 'tonic' IFNAR proximal signaling in IRF9-, compared to STAT2- or STAT1-, deficiency. However, when studies were conducted in (non-transformed) iPS-macrophages, this phenotype was not observed. Furthermore, the basal transcriptome of STAT2$^{-/-}$ and IRF9$^{-/-}$ macrophages was indistinguishable. It remains to be determined whether apparent clinical differences in the inflammatory disease manifestations of IRF9 deficiency and STAT2 deficiency are mirrored by truly distinct molecular mechanisms.

An interesting aspect beyond the scope of this study is the transcriptional regulation in STAT1$^{-/-}$ cells which we used mainly as a negative control for IFNγ-treatment. Although a complete ISGF3 complex cannot be formed in the absence of STAT1, the transcriptional profile of

Journal Pre-proof

STAT1$^{-/-}$ macrophages treated with IFNα2b was qualitatively similar to that of WT cells and some expression of antiviral proteins like MX1, RSAD2 and ISG15 was noted. In murine *Stat1*$^{-/-}$ bone-marrow derived macrophages, a similar delayed upregulation of *MX1* and *ISG15* transcripts, absent from STAT2- and IRF9-deficient cells, had been noted earlier(31) and attributed to a complex of IRF9 and STAT2 that can bind a subset of ISRE sites(24,37). Furthermore, retained although low level USP18 expression in our STAT1$^{-/-}$ cells is consistent with residual negative regulation of IFNAR signaling despite the lack of ISGF3. Nevertheless, inflammatory disease manifestations fulfilling HLH criteria have also been recognized in STAT1 deficiency(38) as well as IFNAR1(14) and IFNAR2(39) deficiency states, clearly arguing for the involvement of signaling cascades other than IFN-I in the pathogenesis of HLH. In summary, our data clearly demonstrate unrestrained and aberrant IFNAR signaling in STAT2$^{-/-}$ and IRF9$^{-/-}$ cells in response to IFNα2b. IFN-I is induced in response to viral infection or live-attenuated viral vaccination and contributes to innate immune antiviral restraint. Failure to contain viral replication, well-documented for example in STAT2 deficiency(10), might provoke excessive and prolonged IFN-I production, in turn driving aberrant IFNγ-like inflammatory responses. Although paradoxical at first sight, our data suggest the potential use of JAK inhibitors to terminate the dysregulated IFN-I response in order to limit immunopathology in this subgroup, as in other patients with HLH(40).

Journal Pre-proof

Acknowledgements:

We thank Angela Grainger for excellent technical assistance as well as Cathy Browne for expert assistance with iPS cell culture.

Data availability:

The Nanostring dataset generated and analysed during the current study is available from the corresponding author on request.

Author contributions:

FG, JS, CFH, HG, CJAD and TS did experiments and analysed data. SAC and WJ provided iPS lines and techniques. AR, AS, FH and HTR provided patient samples and clinical care. CJAD and SH jointly supervised experiments. FG, CJAD and SH designed the study and drafted the manuscript. All authors revised the manuscript and approved the submitted version.

References:

1. Duncan CJA, Randall RE, Hambleton S. Genetic Lesions of Type I Interferon Signalling in Human Antiviral Immunity. Trends Genet. 2021;37(1):46–58.
2. Duncan CJA, Thompson BJ, Chen R, Rice GI, Gothe F, Young DF, et al. Severe type I interferonopathy and unrestrained interferon signaling due to a homozygous germline mutation in STAT2. Sci Immunol. 2019;4(42).
3. Gruber C, Martin-Fernandez M, Ailal F, Qiu X, Taft J, Altman J, et al. Homozygous STAT2 gain-of-function mutation by loss of USP18 activity in a patient with type I interferonopathy. J Exp Med. 2020;217(5):1–11.
4. Zhang X, Bogunovic D, Payelle-Brogard B, Francois-Newton V, Speer SD, Yuan C, et al. Human intracellular ISG15 prevents interferon-α/β over-amplification and auto-inflammation. Nature. 2015;517(7532):89–93.

Journal Pre-proof

5. Meuwissen MEC, Schot R, Buta S, Oudesluijs G, Tinschert S, Speer SD, et al. Human USP18 deficiency underlies type 1 interferonopathy leading to severe pseudo-TOR CH syndrome. J Exp Med. 2016;213(7):1163–74.

6. Dupuis S, Jouanguy E, Al-Hajjar S, Fieschi C, Zaid Al-Mohsen I, Al-Jumaah S, et al. Impaired response to interferon-α/β and lethal viral disease in human STAT1 deficiency. Nat Genet. 2003;33(3):388–91.

7. Hambleton S, Goodbourn S, Young DF, Dickinson P, Mohamad SMB, Valappil M, et al. STAT2 deficiency and susceptibility to viral illness in humans. Proc Natl Acad Sci U S A. 2013;110(8):3053–8.

8. Hernandez N, Melki I, Jing H, Habib T, Huang SSY, Danielson J, et al. Life-threatening influenza pneumonitis in a child with inherited IRF9 deficiency. J Exp Med. 2018;215(10):2567–85.

9. Bravo García-Morato M, Calvo Apalategi A, Bravo-Gallego LY, Blázquez Moreno A, Simón-Fuentes M, Garmendia J V., et al. Impaired control of multiple viral infections in a family with complete IRF9 deficiency. J Allergy Clin Immunol. 2019;144(1):309-312.e10.

10. Moens L, Van Eyck L, Jochmans D, Mitera T, Frans G, Bossuyt X, et al. A novel kindred with inherited STAT2 deficiency and severe viral illness. J Allergy Clin Immunol. 2017;139(6):1995-1997.e9.

11. Alosaimi MF, Maciag MC, Platt CD, Geha RS, Chou J, Bartnikas LM. A novel variant in STAT2 presenting with hemophagocytic lymphohistiocytosis. J Allergy Clin Immunol. 2019;144(2):611-613.e3.

12. Burns C, Cheung A, Stark Z, Choo S, Downie L, White S, et al. A novel presentation of homozygous loss-of-function STAT-1 mutation in an infant with hyperinflammation—A case report and review of the literature. J Allergy Clin Immunol Pract. 2016;4(4):777–9.

Journal Pre-proof

13. Boehmer DFR, Koehler LM, Magg T, Metzger P, Rohlfs M, Ahlfeld J, et al. A Novel Complete Autosomal-Recessive STAT1 LOF Variant Causes Immunodeficiency with Hemophagocytic Lymphohistiocytosis–Like Hyperinflammation. J Allergy Clin Immunol Pract. 2020;8(9):3102–11.

14. Gothe F, Hatton CF, Truong L, Klimova Z, Kanderova V, Fejtkova M, et al. A Novel Case of Homozygous Interferon Alpha/Beta Receptor Alpha Chain (IFNAR1) Deficiency With Hemophagocytic Lymphohistiocytosis. Clin Infect Dis. 2020;Nov 30(Online ahead of print).

15. Jordan MB, Hildeman D, Kappler J, Marrack P. An animal model of hemophagocytic lymphohistiocytosis (HLH): CD8 + T cells and interferon gamma are essential for the disorder. Blood. 2004;104(3):735–43.

16. Haenseler W, Zambon F, Lee H, Vowles J, Rinaldi F, Duggal G, et al. Excess α-synuclein compromises phagocytosis in iPSC-derived macrophages. Sci Rep. 2017;7(1):1–11.

17. van Wilgenburg B, Browne C, Vowles J, Cowley SA. Efficient, Long Term Production of Monocyte-Derived Macrophages from Human Pluripotent Stem Cells under Partly-Defined and Fully-Defined Conditions. PLoS One. 2013;8(8).

18. Ho Sui SJ, Mortimer JR, Arenillas DJ, Brumm J, Walsh CJ, Kennedy BP, et al. oPOSSUM: Identification of over-represented transcription factor binding sites in co-expressed genes. Nucleic Acids Res. 2005;33(10):3154–64.

19. Kamburov A, Stelzl U, Lehrach H, Herwig R. The ConsensusPathDB interaction database: 2013 Update. Nucleic Acids Res. 2013;41(D1):793–800.

20. Carbon S, Douglass E, Good BM, Unni DR, Harris NL, Mungall CJ, et al. The Gene Ontology resource: Enriching a GOld mine. Nucleic Acids Res. 2021;49(D1):D325–34.

21. Gough DJ, Messina NL, Clarke CJP, Johnstone RW, Levy DE. Constitutive Type I

Journal Pre-proof

Interferon Modulates Homeostatic Balance through Tonic Signaling. Immunity. 2012;36(2):166–74.

22. Malakhova OA, Kim K Il, Luo JK, Zou W, Kumar KGS, Fuchs SY, et al. UBP43 is a novel regulator of interferon signaling independent of its ISG15 isopeptidase activity. EMBO J. 2006;25(11):2358–67.

23. Platanitis E, Demiroz D, Schneller A, Fischer K, Capelle C, Hartl M, et al. A molecular switch from STAT2-IRF9 to ISGF3 underlies interferon-induced gene transcription. Nat Commun [Internet]. 2019;10(1):2921. Available from: http://dx.doi.org/10.1038/s41467-019-10970-y

24. Blaszczyk K, Olejnik A, Nowicka H, Ozgyin L, Chen YL, Chmielewski S, et al. STAT2/IRF9 directs a prolonged ISGF3-like transcriptional response and antiviral activity in the absence of STAT1. Biochem J. 2015;466(3):511–24.

25. Majumder S, Zhou LZ, Chaturvedi P, Babcock G, Aras S, Ransohoff RM. p48/STAT-1alpha-containing complexes play a predominant role in induction of IFN-gamma-inducible protein, 10 kDa (IP-10) by IFN-gamma alone or in synergy with TNF-alpha. J Immunol. 1998;161(9):4736–44.

26. Kershaw NJ, Murphy JM, Liau NPD, Varghese LN, Laktyushin A, Whitlock EL, et al. SOCS3 binds specific receptor-JAK complexes to control cytokine signaling by direct kinase inhibition. Nat Struct Mol Biol. 2013;20(4):469–76.

27. Goldmann T, Zeller N, Raasch J, Kierdorf K, Frenzel K, Ketscher L, et al. USP 18 lack in microglia causes destructive interferonopathy of the mouse brain . EMBO J. 2015;34(12):1612–29.

28. Song MM, Shuai K. The suppressor of cytokine signaling (SOCS) 1 and SOCS3 but not SOCS2 proteins inhibit interferon-mediated antiviral and antiproliferative activities. J Biol Chem. 1998;273(52):35056–62.

29. Qiao Y, Giannopoulou EG, Chan CH, Park S ho, Gong S, Chen J, et al. Synergistic

Journal Pre-proof

activation of inflammatory cytokine genes by interferon-γ-induced chromatin remodeling and toll-like receptor signaling. Immunity. 2013;39(3):454–69.

30. Zhao W, Cha EN, Lee C, Park CY, Schindler C. Stat2-Dependent Regulation of MHC Class II Expression. J Immunol. 2007;179(1):463–71.

31. Abdul-Sater A, Majoros A, Plumlee1 C, Perry S, Gu A, Lee C, et al. Different STAT transcription complexes drive early and delayed responses to type I Interferons. J Immunol. 2015;195(1):210–6.

32. Li W, Hofer MJ, Songkhunawej P, Jung SR, Hancock D, Denyer G, et al. Type I interferon-regulated gene expression and signaling in murine mixed glial cells lacking signal transducers and activators of transcription 1 or 2 or interferon regulatory factor 9. J Biol Chem. 2017;292(14):5845–59.

33. Piganis RAR, De Weerd NA, Gould JA, Schindler CW, Mansell A, Nicholson SE, et al. Suppressor of Cytokine Signaling (SOCS) 1 inhibits type I interferon (IFN) signaling via the interferon α receptor (IFNAR1)-associated tyrosine kinase tyk2. J Biol Chem. 2011;286(39):33811–8.

34. Hadjadj J, Castro CN, Tusseau M, Stolzenberg MC, Mazerolles F, Aladjidi N, et al. Early-onset autoimmunity associated with SOCS1 haploinsufficiency. Nat Commun. 2020;11(1):1–11.

35. Arimoto KI, Miyauchi S, Stoner SA, Fan JB, Zhang DE. Negative regulation of IFN-I signaling. J Leukoc Biol. 2018;103(6):1099–116.

36. Taylor JP, Cash MN, Santostefano KE, Nakanishi M, Terada N, Wallet MA. CRISPR/Cas9 knockout of USP18 enhances IFN-I responsiveness and restricts HIV-1 infection in macrophages. J Leukoc Biol. 2018;103(6):1225–40.

37. Bluyssen HAR, Levy DE. Stat2 is a transcriptional activator that requires sequence-specific contacts provided by Stat1 and p48 for stable interaction with DNA. J Biol Chem. 1997;272(7):4600–5.

Journal Pre-proof

38. Le Voyer T, Sakata S, Tsumura M, Khan T, Esteve-Sole A, Al-Saud BK, et al. Genetic, Immunological, and Clinical Features of 32 Patients with Autosomal Recessive STAT1 Deficiency. J Immunol. 2021;207(1):133–52.

39. Passarelli C, Civino A, Rossi MN, Cifaldi L, Lanari V, Moneta GM, et al. IFNAR2 Deficiency Causing Dysregulation of NK Cell Functions and Presenting With Hemophagocytic Lymphohistiocytosis. Front Genet. 2020;11(September):1–6.

40. Chinn IK, Eckstein OS, Peckham-Gregory EC, Goldberg BR, Forbes LR, Nicholas SK, et al. Genetic and mechanistic diversity in pediatric hemophagocytic lymphohistiocytosis. Blood. 2018;132(1):89–100.

Figure legends:

Fig 1. Prolonged IFNAR signaling and failure to upregulate USP18. Time course of IFNα2b stimulation (1000 IU/mL) in EBV-LCLs from patients and controls (a) Immunoblot; repeat experiments n=3 (b) Representative histograms (Flow cytometry) with mean fluorescence intensity (MFI) of (c) pSTAT1 and (d) pSTAT2 over time; n= 4 (e) *USP18* mRNA expression over time measured by RT-qPCR; n=3. Data are shown as mean ± SEM (* p<.05, ** p<.01, *** p<.001, **** p<.0001, one-way ANOVA with Tukey correction for multiple comparisons).

Fig. 2. Failure to induce classical ISGs and heightened expression of GAS-controlled genes. RT-qPCR analysis of ISGs in response to IFNα2b stimulation (1000 IU/mL) for the indicated times. Expression of classical antiviral genes (a) *MX1*, (b) *RSAD2*, (c) *IFI44L*. Induction of

Journal Pre-proof

known IFNγ-activated genes (d) *IRF1* (e) *CIITA*, (f) *ICAM1*; repeat experiments n=3-4. Data are presented as means ± SEM (* p<.05, ** p<.01, *** p<.001, **** p<.0001, one-way ANOVA with Tukey correction for multiple comparisons).

Fig. 3. Validation of the iPS-derived KO macrophage lines. (a) Immunoblot of wild-type and KO iPS-macrophage lines stimulated with IFNα2b (1000 IU/mL) or left untreated; Repeat experiments n=3 (b) Representative flow cytometry histograms of iPS-macrophage surface marker expression. The dotted line indicates isotype controls (c) Phagocytosis assay comparing fluorescent bead uptake at 37°C versus 4°C (dotted line, negative control); repeat experiments n=2.

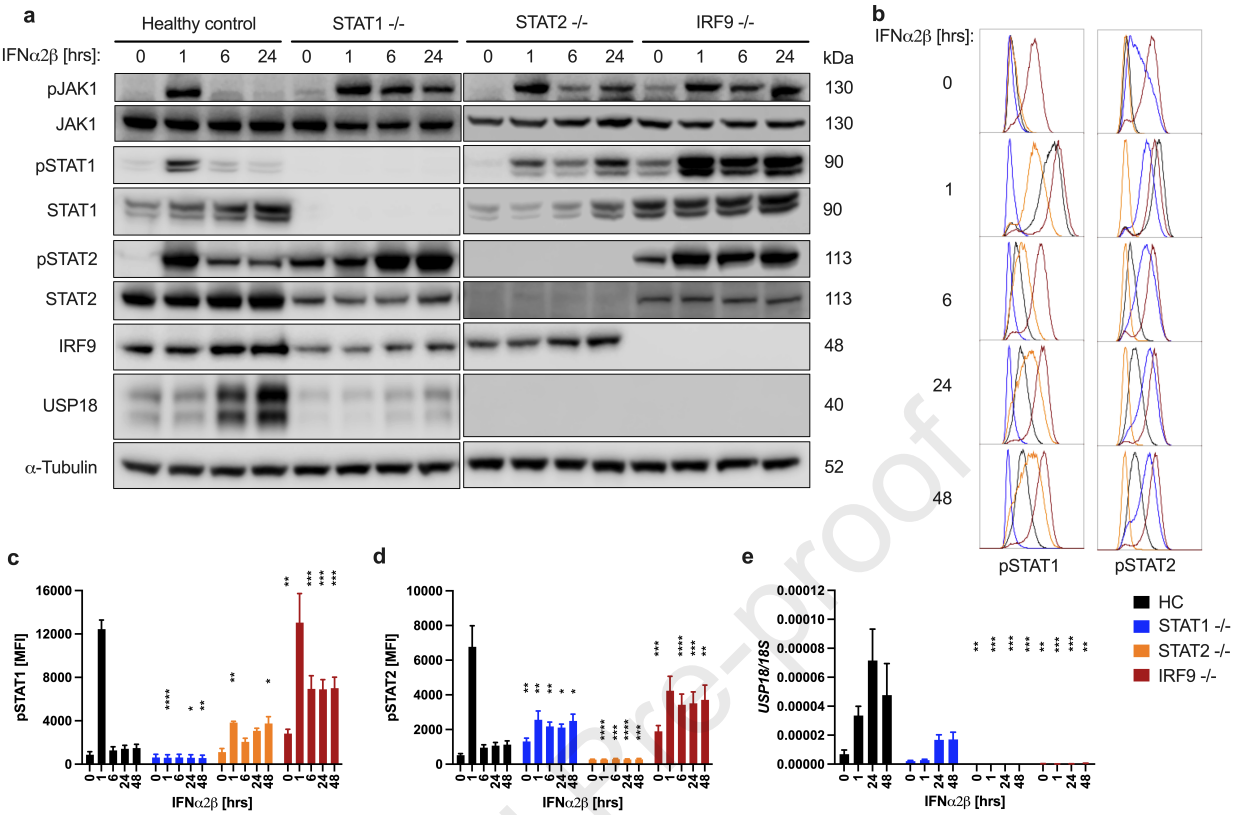
Fig. 4. Transcriptional changes in iPS-derived KO macrophages following IFN stimulation. (a) ISG induction following IFNα2b stimulation (1000 IU/mL) for 1hr in WT, STAT1$^{-/-}$, STAT2$^{-/-}$ and IRF9$^{-/-}$ iPS-macrophages on an isogenic background. Only the genes with >1.5 fold induction in both WT lines are displayed. (b) Fold changes between 1 hr and 48 hrs of IFNα stimulation analyzing the genes used in a. Log_2 transformed data are shown. (c) PCA analysis of samples after 48 hrs of IFNα2b or IFNγ stimulation (1000 IU/mL each). PCA1 accounts for 46% of the variability, PC2 for 19% (square: unstimulated; circle: IFNα2b; triangle: IFNγ). (d) Venn diagrams shows numbers of differentially expressed genes with predicted binding sites for the indicated transcription factors ISGF3 or GAF and IRF1 within 1,000 bp of their promoter sequence for WT, STAT2$^{-/-}$ and IRF9$^{-/-}$ iPS-macrophages following 48 hrs of IFNα2b stimulation.

Fig. 5. Macrophage activation in response to IFN stimulation. Upregulation of surface markers (a) HLA-DR, (b) ICAM1 and (c) IRF1 in iPS-macrophages following stimulation with 1000 IU/mL IFNα2b or IFNγ. Repeat experiments n=3. (d) Flow cytometric analysis of intracellular

Journal Pre-proof

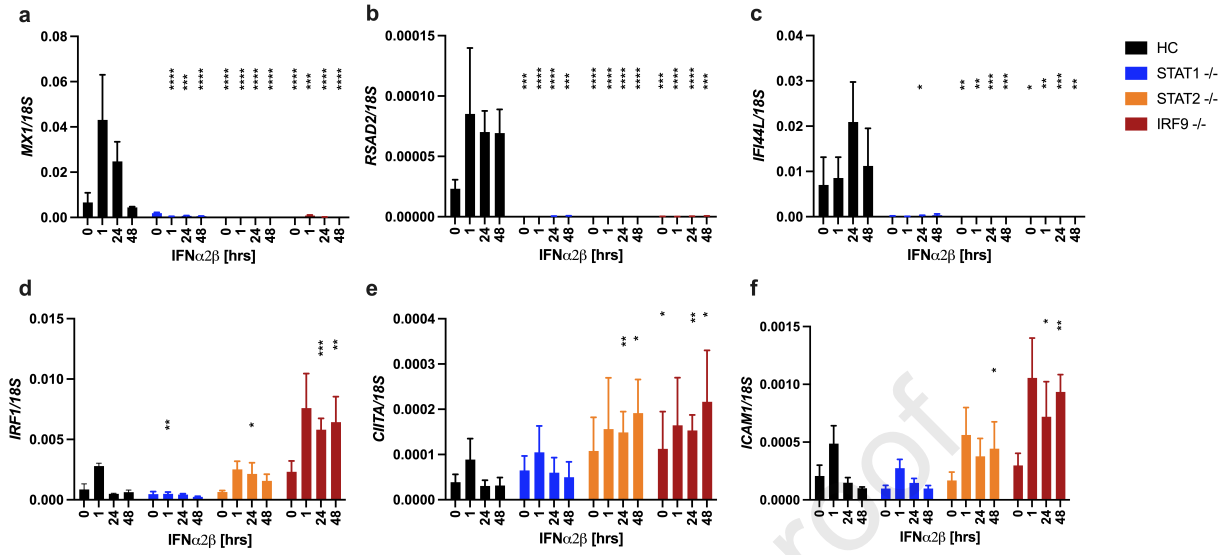
TNFα accumulation. Cells were primed with IFNα2b or IFNγ for 48 hrs before LPS (100 ng/mL) was added as a second stimulus. Repeat experiments n=3. Data are presented as mean ± SEM (* p<.05, ** p<.01, *** p<.001, **** p<.0001, one-way ANOVA with Tukey correction for multiple comparisons).

Journal Pre-proof

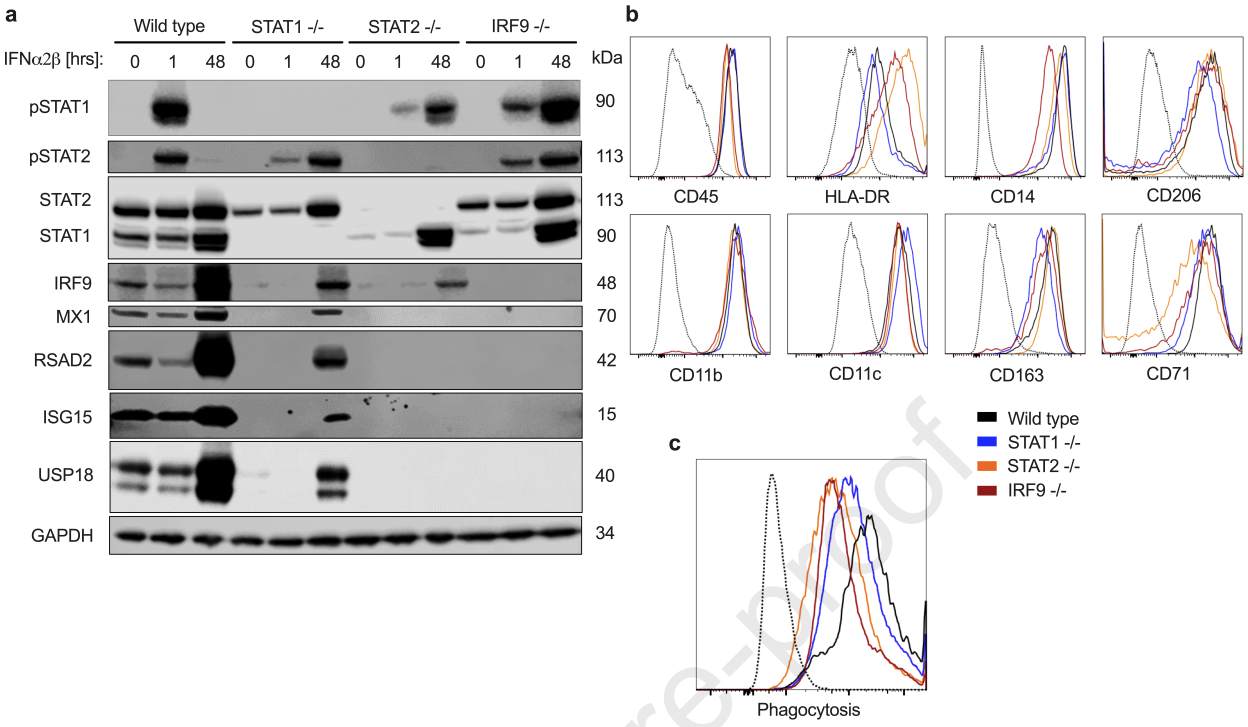


Journal Pre-proof

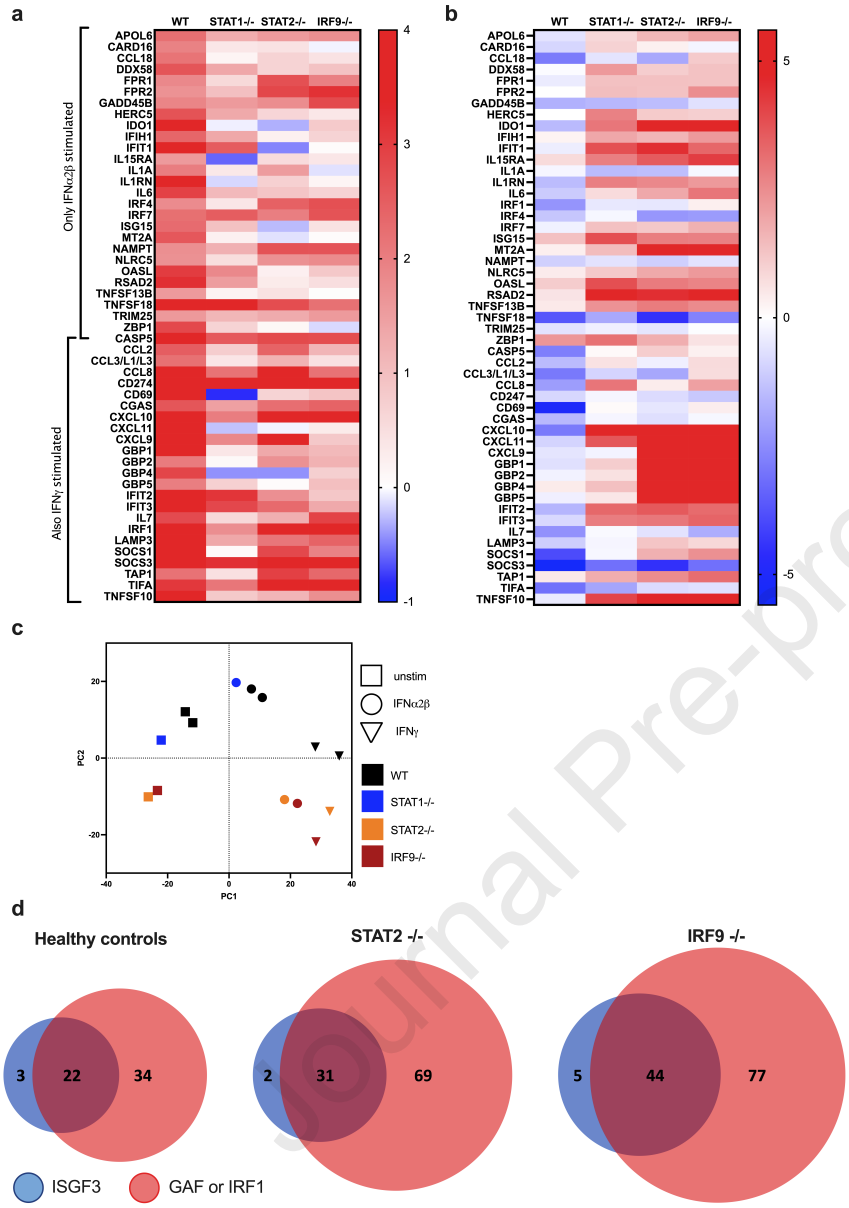
Journal Pre-proof



Journal Pre-proof

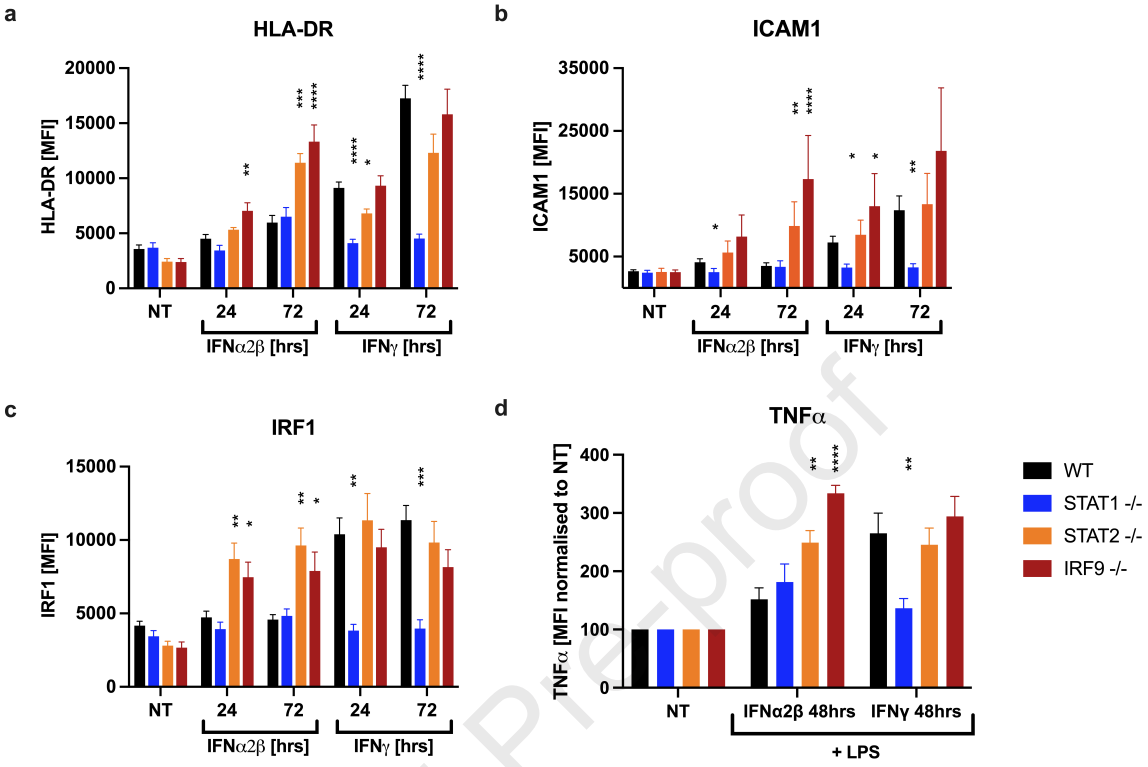


Journal Pre-proof



Journal Pre-proof

Journal Pre-proof



Journal Pre-proof

Journal Pre-proof

Supplementary figure legends:

Fig. S1. Gating strategies in (a) EBV-LCLs and (b) iPS-derived macrophages.

Fig. S2. Coimmunoprecipitation of (a) STAT1 and (b) STAT2 in EBV-LCLs stimulated with IFNα2b (1000 IU/mL) for 15 minutes. Representative images from 3-4 independent experiments.

Fig. S3. RT-qPCR analysis of (a) *SOCS1* and (b) *SOCS3* in response to IFNα2b stimulation (1000 IU/mL) for the indicated times. Repeat experiments n=3-4. Data are presented as means ± SEM (* $p<.05$, ** $p<.01$, one-way ANOVA with Tukey correction for multiple comparisons). (c) STAT1 phosphorylation in response to IFNγ following different IFNα2b priming intervals.

Fig. S4. Expression of (a) ICAM1, (b) IRF1, and (c) HLA-DR in EBV-LCLs following 48 hrs of IFNα2b stimulation (1000 IU/mL).

Fig. S5. Verification of ISGF3 component knockouts in iPS-derived macrophages. (a) Sequence analysis of different iPSC clones following gene editing. IRF9 protein expression could not be detected in iPSCs. Confirmation of complete knockout of (b) STAT1 and (c) STAT2 in iPSC cells after gene editing. (d) Complete absence of residual protein expression after differentiation into macrophages; Number of repeat Western blot experiments in macrophages n=3.

Fig. S6. Differential gene expression at baseline in (a) $STAT1^{-/-}$, (b) $STAT2^{-/-}$ and (c) $IRF9^{-/-}$ iPS-macrophages. Genes with a 10X increase or decrease compared to WT cells are labelled. Colours indicate the transcriptional influence of certain IFNs (purple: IFNα2b; blue: IFNα2b

Journal Pre-proof

and IFNγ; green: IFNβ; red: IFNγ; grey: not induced >2fold; black: not found) based on the Interferome database (v2.01, Monash University, Australia).

Fig. S7. ISG induction following IFNγ stimulation (1000 IU/mL) for 1hr in WT, STAT1$^{-/-}$, STAT2$^{-/-}$ and IRF9$^{-/-}$ macrophages on an isogenic background. Only the genes with >1.5 fold induction in both WT lines are displayed.

Fig. S8. Pathway analysis after 48 hrs of stimulation with IFNα2b (1000 IU/mL), displaying the top 10 GO terms induced in STAT2$^{-/-}$ and IRF9$^{-/-}$ iPS macrophages.

Fig. S9. Transcriptional induction of cytokines relevant to HLH pathogenesis in iPS-derived macrophages stimulated with IFNα2b (1000 IU/mL) for 48 hrs.

Fig. S10. Intracellular IL-6 accumulation in iPS-derived macrophages primed for 48 hrs with either IFNα2b or IFNγ (1000 IU/mL each) before being treated with LPS.

Fig. S11. Expression of (a) ICAM1, (b) IRF1, and (c) HLA-DR in EBV-LCLs pretreated with either IL-4, IL-5, or IL-15 (50 ng/mL each) or 10 uM Dexamethasone overnight before being stimulated with IFNα2b (1000 IU/mL) for 48 hrs. Blockade of type I IFN-induced upregulation of (d) ICAM1, (e) IRF1, and (f) HLA-DR expression by ruxotinib (1 uM) pretreatment.

Journal Pre-proof